

The High Density Effects in Heavy Quark Production at pA Colliders

A. L. Ayala Filho ^{1,*} and *V. P. Gonçalves* ^{1,2,**}

¹ *Instituto de Física e Matemática, Univ. Federal de Pelotas
Caixa Postal 354, 96010-090, Pelotas, RS, BRAZIL*

² *Universidade Estadual do Rio Grande do Sul - UERGS,
Borges de Medeiros, 1501, 90119-900, Porto Alegre, RS, BRAZIL*

Abstract: In this paper we investigate the role of the high density effects in the heavy quark production cross section in pA processes at RHIC and LHC. We use, as initial condition, a gluon distribution consistent with fixed target nuclear data and the Glauber-Mueller approach to describe the high density effects. We show that this process can be used as a probe of the presence of the high density effects. Moreover, we include these effects in the calculation of the heavy quark production in AA collisions, verifying that they cannot be disregarded both in the estimates of quarkonium suppression and in the initial conditions of the quark-gluon plasma.

PACS numbers: 11.80.La; 24.95.+p;

Key-words: Small x QCD; High Density Effects; Nuclear Collisions.

^{0*}E-mail:ayala@ufpel.tche.br

^{0**}E-mail:barros@ufpel.tche.br

The relativistic collider facilities RHIC and LHC will for the first time provide the opportunity to systematically study the physics of hot and ultra-dense matter in hadron-nucleus (pA) and nucleus-nucleus (AB) collisions at energies that are orders of magnitude larger than the energies of the current accelerators. The systematic study of pA collisions at the same energies is essential to gain insight into the structure of the dense medium effects. Such effects, as the energy loss and shadowing, are absent or small in pp collisions, but become increasingly prominent in pA collisions, and are of major importance in AA reactions. By comparing pA and AA reactions involving very heavy nuclei, one may be able to distinguish basic hadronic effects that dominate the dynamics in pA collisions, from a quark-gluon formation predicted to occur in heavy ion AA collisions. To gain insight into the underlying hadronic processes, one has to study collisions that are expected to not lead to a QGP formation. Once the physics of "QCD at high densities" is better understood, the mechanisms of quark-gluon plasma formation and related collective phenomena in heavy ion collisions could be disentangled from the basic hadronic effects.

One of the nuclear medium effects is the nuclear shadowing, which is the modification of the target parton distributions so that $xq^A(x, Q^2) < Axq^N(x, Q^2)$, as expected from a superposition of pp interactions. The current experimental data presenting nuclear shadowing can be described reasonably using the DGLAP evolution equations [1] with adjusted initial parton distributions [2]. However, this parameterization does not include the dynamical saturation effects of the parton distributions predicted at small x and large A [3]. In this kinematical regime, the density of quarks and gluons becomes very high and the processes of interaction and recombination between partons, not present in the DGLAP evolution, should be considered. Recently, we have proposed a procedure to improve the nuclear parton distributions and include the perturbative high density effects in the predictions of the inclusive observables in eA processes [4]. There we have indicate that the high density effects becomes very important mainly for the LHC kinematic region and that these effects could not be disregarded in the calculations of the observables and signatures of the QGP. Here we analyze in detail the heavy quark production in pA processes in order to investigate the presence and magnitude of the high density effects (For a related discussion of heavy quark production see Refs. [5, 6]). Our analyzes is motivated by the fact that the heavy quark production at RHIC and LHC energies is dominated by

initial state gluons. Thus, the pA process becomes a valuable search of information about the gluon distribution in the nucleus. Since the probability for making a heavy quark pair is proportional to square of gluon distribution, any depletion in number of gluons will make a significant difference in the number of heavy quark pairs produced.

Lets start from a brief review of the high density scenario. At high densities we expect the limitation on the maximum phase-space parton density that can be reached in the hadron wavefunction (parton saturation) and very high values of the QCD field strength squared $F_{\mu\nu}^2 \propto 1/\alpha_s$ [3], possibly forming a Color Glass Condensate [8], which is characterized by a bulk momentum scale Q_s . If this saturation scale is larger than the QCD scale Λ_{QCD} , then this system can be studied using weak coupling methods. At present, there are different approaches to describe hdQCD effects, all of them including nonlinear terms in parton evolution equations [9]. In fact, these approaches sum powers of the probability of gluon-gluon interaction inside of the parton cascade. As a summary, we have that the different approaches match the DLA limit of the DGLAP parton evolution in the low parton density limit and match the Glauber-Mueller approach in the transition regime of low density to the high density limit. At the energies of interest, we believe that the predictions of the Glauber-Mueller approach can be taken as good approximation to the description of high density effects. As this approach is a common limit to the distinct approaches, we intend to obtain predictions which are not model dependent.

The main properties of the nuclear gluon distribution $xG^A(x, Q^2)$ in the Glauber-Mueller approach were extensively discussed in Ref. [10]. For completeness, we now present a qualitative discussion of the main properties of this approach. In the nucleus rest frame we can consider the interaction between a virtual colorless hard probe and the nucleus via the gluon pair (gg) component of the virtual probe. The interaction of the dipole with the color field of the nucleus will clearly depend on the size of the dipole. If the separation of the gg pair is very small (smaller than the mean separation of the partons), the color field of the dipole will be effectively screened and the nucleus will be essentially 'transparent' to the dipole. At large dipole sizes, the color field of the dipole is large and it interacts strongly with the target and is sensitive both to its structure and size. More generally, when the parton density is such that the nucleus becomes 'black' and the interaction probability is unity, the dipole cross section saturates and the gluon distribu-

tion becomes proportional to the virtuality of the probe Q^2 . In the infinite momentum frame, this picture is equivalent to a situation in which the individual partons become so close that they have a significant probability of interacting with each other before interaction with the probe. Such interactions lead, for instance, to two \rightarrow one branchings and hence a reduction in the gluon distribution. These properties were considered in Ref. [10], where the rescatterings of the gluon pair inside the nucleus were estimated using the Glauber-Mueller approach, resulting that the nuclear gluon distribution is given by [10]

$$xG_A(x, Q^2) = \frac{2R_A^2}{\pi^2} \int_x^1 \frac{dx'}{x'} \int_{\frac{1}{Q^2}}^{\frac{1}{Q^2}} \frac{d^2 r_t}{\pi r_t^4} \{C + \ln(\kappa_G(x', r_t^2)) + E_1(\kappa_G(x', r_t^2))\} \quad (1)$$

where C is the Euler constant, E_1 is the exponential function, the function $\kappa_G(x, r_t^2) = (3\alpha_s A/2R_A^2) \pi r_t^2 x G_N(x, \frac{1}{r_t^2})$, A is the number of nucleons in a nucleus and R_A^2 is the mean nuclear radius. One of the shortcomings of this approach is that the Glauber-Mueller formula disregards any nuclear effect in the nonperturbative initial condition for the gluon distribution. Furthermore, the medium effects present at larger values of x , the antishadowing and the EMC effect, are also disregarded in this approach. In order to improve the Glauber-Mueller approach, it was recently proposed in Ref.[4] a modification in the expression (1) that includes the full DGLAP kernel in parton evolution. Basically, we propose to calculate the nuclear gluon distribution using the following procedure:

$$\begin{aligned} xG_A(x, Q^2) = & (1/A)xG_A(x, Q^2)[GM] - (1/A)xG_A(x, Q^2)[DLA] \\ & + xG_A(x, Q^2)[EKS] , \end{aligned} \quad (2)$$

where $xG_A(x, Q^2)[GM]$ represents the Glauber-Mueller nuclear gluon distribution given by the expression (1) and $xG_A(x, Q^2)[DLA]$ is the DGLAP (DLA) prediction for the nuclear gluon distribution, which correspond to the first term of expression (1) when expanded in powers of κ_G . The last term in expression (2), $xG_A(x, Q^2)[EKS]$, is the gluon distribution solution of the DGLAP equation as proposed by Eskola, Kolhinen and Salgado(EKS) [2], where the initial conditions of the parton evolution are chosen in such a way to describe the nuclear effects in DIS and Drell-Yan fixed nuclear target data. As it was discussed in detail in Ref.[4], the parameterization of the nuclear effects in the gluon distribution, given by the ratio

$R_G^A(x, Q^2) = xG_A(x, Q^2)/xG_N(x, Q^2)$ in the EKS procedure, does not include the perturbative high density effects at small values of x . Thus, the procedure presented in equation (2) includes the full DGLAP evolution equation in all kinematic region, take into account the nuclear affect in the present fixed target data and includes the high density effects in the parton evolution at small x in the perturbative regime.

To illustrate our results, in Fig. 1 we compare our predictions for the x - dependence of the ratio $R_G = xG_A/xG_N$ for $Q^2 = 15$ GeV 2 with the EKS predictions. The results are shown for two typical nuclei of interest in nuclear collisions. Also the corresponding kinematic region which will be explored in the RHIC and LHC colliders are presented. Two important features of the high density effects can be seen in Fig. 1: the magnitude of the effects and the saturation behavior. The suppression of the gluon distribution in respect to the EKS set is 6% for $A=40$ (Ca) and 11% for $A=208$ (Pb) in the lower limit of the RHIC kinematic range. When the lower limit of the LHC kinematic range is concerned, the reduction of the gluon distribution is 31% for $A=40$ and 50% for $A=208$. This strong effect also modify the saturation of the ratio predicted in the EKS parameterization at low x . Basically, in the EKS approach the saturation of the ratio is assumed in the nonperturbative initial condition as a constraint for the behavior of the nuclear parton distributions in the small x limit. This behavior is preserved by the DGLAP evolution, since these equations reduce to the DLA limit at low x in the nucleon and nuclear case, keeping the ratio constant. When the high density effects are considered in the dynamics, a large modification of the gluon distribution is predicted, which is amplified in nuclear processes since the nuclear medium amplifies the effects associated to the high parton density. Therefore, the high density approaches predict larger effects in the nuclear gluon distribution than the nucleon one, independent of the initial parton distributions used. This expectation is present in the behavior of $R_G^A(AG)$, which turn to be much smaller then $R_G^A(EKS)$ in low x region. As the heavy quark production is dominated by the fusion of gluons, we expect that these effects will strongly modify the $c\bar{c}$ and $b\bar{b}$ production in pA processes in the high energy limit.

Now let us consider the heavy quark production. Perturbative QCD calculations of heavy quark production at leading order have long been available. For high energies and at leading order (LO), the production is dominated by gluon fusion, with charm and bottom quarks produced basically in the pro-

cess $gg \rightarrow Q\bar{Q}$ with $Q = c$ and b . The LO cross section for a proton p colliding with a nucleus A is then:

$$\sigma_{pA} = \int d\tau \int dx_F \frac{1}{s} \frac{1}{\sqrt{x_F^2 + 4\tau}} xG_p(x_1, \mu^2) xG_A(x_2, \mu^2) \times \hat{\sigma}_{gg \rightarrow Q\bar{Q}}(x_1, x_2, m_Q, \mu^2), \quad (3)$$

where $x_F = x_1 - x_2$, $\tau = M^2/s$ and M^2 is the invariant mass of the virtual gluon in the subprocess. xG_i the gluon distributions evaluated at momentum fraction x and momentum scale μ^2 . For practical purpose, we take $\mu^2 = 4m_c^2$ for charm production and $\mu^2 = m_b^2$ for bottom production. In order to investigate the medium dependence of the heavy quark production cross section, we will follow the usual procedure used to describe the experimental data on nuclear effects in the hadronic quarkonium production [12], where the atomic mass number A dependence is parameterized by $\sigma_{pA} = \sigma_{pN} \times A^\alpha$. Here σ_{pA} and σ_{pN} are the particle production cross sections in proton-nucleus and proton-nucleon interactions, respectively. If the particle production is not modified by the presence of nuclear matter, then $\alpha = 1$. A number of experiments have measured a less than linear A dependence for various processes of production, which indicates that the medium effects cannot be disregarded. As our focus is to analyze the influence of the high density effects in the heavy quark production when compared to the usual DGLAP-EKS predictions, we do not consider the contributions of energy loss and the intrinsic heavy-quark components for the non-linear A dependence of the cross sections (For a discussion of these effects in charmonium production see Ref. [13]). In this paper we will evaluate the heavy quark production at leading order and will use the quark masses $m_c = 1.2$ GeV and $m_b = 4.75$ GeV. To estimate the modification of heavy quark production cross section due to the high density effects, we calculate the effective exponent α , which is given by

$$\alpha = \left(\ln \frac{\sigma_{pA}}{\sigma_{pN}} \right) / \ln A. \quad (4)$$

We calculate the above expression considering, as an input in the nuclear cross sections, the parameterization of the nuclear effects in the gluon distributions, which is given by $xG_A(x_i, \mu^2) = R_G(x_i, \mu^2) xG_N(x_i, \mu^2)$, with R_G

presented in Fig. 1 and xG_N taken from the GRV94(LO) set [14]. Two comments are in order here. First, since we are interested in the behavior of the effective exponent, we may expect that our results will not be modified by the NLO corrections (the K -factor) [11]. Second, we are assuming that the collinear factorization is still valid in the kinematic region considered. This is a strong assumption which should be tested by the comparison of our results with a calculation of this process considering the color glass condensate formalism, similarly to made in Ref. [18] for photoproduction. The agreement between the results will allow us to use our approach as a simplified method of inclusion of the high density effects in the nuclear cross sections. Furthermore, the comparison between the results of our approach and the color glass predictions for the gluon minijet production [19] will be other important cross check of our approach. Work in this direction is in progress.

In order to gain insight into the amount of the high density effects in heavy quark production at future colliders, we will consider the process calculated at the proposed energies for RHIC and LHC. These energies are $\sqrt{s} = 200$ GeV per nucleon pair for Au+Au collisions and $\sqrt{s} = 350$ GeV for pA process at RHIC. For LHC, $\sqrt{s} = 5500$ GeV per nucleon pair for Pb+Pb collisions and $\sqrt{s} = 8800$ GeV for pA processes [20]. In Fig. 2 we present the effective exponent α as a function of the c.m. energy $s^{1/2}$ for two different nucleus. We verify that the high density effects are sizeable at high values of energy even for a small value of the mass number ($A = 40$). The general behavior of the exponent can be understood as follows. When the integrations in Eq. (3) are taken, the nuclear gluon distribution are evaluated in the x_2 interval given by $\tau < x_2 < \sqrt{\tau}$. Thus, when the energy grows, the x_2 interval goes to the small x region. For charm production, for example, the antishadowing region in Fig. 1 dominates the integration for energies smaller than 80 GeV. For bigger energies, the shadowing region dominates and the exponent is smaller than 1. In bottom production, the x_2 interval is dislocated to larger values of x , which implies that the antishadowing region of Fig. 1 dominates the production at energies in the interval 100-200 GeV and α is close to one even for RHIC energies. For bigger values of energy, the suppression is sizeable and the effective exponent is smaller than 1. In general grounds we have that the saturation of the exponent observed in the EKS prediction is associated to the behavior of the ratio R_G at small x , while the presence of the high density effects (nonsaturation of R_G) implies a large reduction of the

pA cross section when compared with DGLAP-EKS description of nuclear effects. Therefore, we believe that the analyzes of the effective exponent in pA processes can be useful to evidence the high density effects.

In Fig. 3, we present the exponent α for RHIC and LHC energies as a function of $x_F \equiv x_1 - x_2$. The exponent was obtained from the expression

$$\alpha(x_F) = \left\{ \ln \left(\frac{d\sigma_{pA}}{dx_F} \Big/ \frac{d\sigma_{pN}}{dx_F} \right) \Big/ \ln A \right\} , \quad (5)$$

where the differential cross section was obtaining integrating equation (3) in the invariant mass of the virtual gluons from the heavy quark threshold to the energy squared s , which corresponds to $\frac{m_Q^2}{s} < \tau < 1$. For values of x_F close to zero, $x_2 \approx x_1$ and the τ integration corresponds to a large interval in both x_2 and x_1 . For x_F close to one, both x_2 and x_1 interval are much smaller, with x_1 close to one and x_2 close to zero. The lower limit of τ corresponds also to the lower x_2 limit. Considering the kinematics discussed above and the properties of the Fig. 1, all the features of Fig. 3 can be understood. For the $p - Pb$ processes at RHIC ($\sqrt{s} = 350$ GeV) with x_F close to zero, the exponent is close to one. This occurs because the τ integration corresponds to a large interval in x_2 , including contribution from the antishadowing region of Fig. 1. For charm production, the threshold is low enough to include the contribution from the small x_2 region and the exponent α is smaller than one. For the bottom production, the low x_2 contribution is small and the exponent is bigger than one. Since high density effects are small in the intermediate x_2 region, the EKS and AG prediction are close to each other. For x_F close to one, the low x_2 behavior of the gluon distribution dominates the process. Since the EKS parameterization predicts that the ratio saturates at this region, the exponent tend to a constant, while the high density effects predict an exponent that decrease monotonically. These effects are much stronger in the charm production due to the lower threshold. Moreover, all effects discussed above are amplified for LHC energy ($\sqrt{s} = 8.8$ TeV), even for x_F close to zero. Due to the large energy, the lower limit of the τ integration is very close to zero. Then, the low x_2 contribution is much bigger and the high density effects are much more important. For x_F close to one, the EKS prediction indicates a constant value for α , both for charm and bottom production. This is a direct consequence of the saturation of the ratio R_G in the low x_2 region. As far as the high density effects are

considered, the exponent is strongly reduced. As x_F tend to one, α goes to 0.6 for charm production and 0.7 for bottom production.

The strong modification of the heavy quark production in pA process indicate that high density effects on the gluon distribution will play an important role in the calculation of the initial conditions and signatures of the quark-gluon plasma in heavy ion collisions. To illustrate this point, we present in Fig. 4 the exponent β calculated by the expression

$$\beta = \left(\ln \frac{\sigma_{AA}}{\sigma_{pN}} \right) / \ln A , \quad (6)$$

for the heavy quark production in Pb-Pb collisions as a function of \sqrt{s} . The exponent present a similar feature to the exponent α shown in Fig. 2. For energies close and smaller than 100 GeV, the most important contribution comes from the antishadowing region of Fig. 1, and the exponent is bigger than two. For larger energies, the small x region gives the more important contribution. When compared to the EKS prediction, the high density effects strongly reduces the production cross sections. At RHIC energy ($\sqrt{s} = 200\text{GeV}$), the exponent β is reduced in 8% for $c\bar{c}$ and 4% for $b\bar{b}$. At LHC energy ($\sqrt{s} = 5500$), the relative reduction is 42% for $c\bar{c}$ and 28% for $b\bar{b}$. As we can see, the high density effects will strongly reduce the production cross sections in AA processes and should be taken into account to calculate the cross section of the hard QCD process in the first stage of the heavy ion collisions.

In brief, a systematic measurement of gluon shadowing is of fundamental interest in understanding of the parton structure of nuclei as well as in the field of minijet production that determines the total entropy produced at RHIC and higher energies. In this paper we addressed the heavy quark production in pA processes as a search to verify the presence and estimate the magnitude of the high density effects and, consequently, fix the behavior of the gluon distribution at large energies. In this sense our results can be considered as complementary to the predictions made by Wang and Gyulassy [21], which have studied the sensitivity of single-particle inclusive spectra in nuclear collisions to gluon shadowing and jet quenching, and have suggested the investigation of the pA collisions at the same energy in order to disentangle both effects. Moreover, the study of heavy quark production is important to estimate the suppression of this process associated to the high

density effects, which is necessary for a reliable calculation of quarkonium production and its suppression in a quark-gluon plasma. As a summary of our results we have calculated the cross sections for heavy quark production in pA processes and estimated the energy and x_F dependencies of the effective exponents that parameterize the medium effects. Our results demonstrate that these effects are large even at small nuclei and that a systematic experimental analyzes could discriminate between the high density regime and the predictions from the linear regime. Furthermore, we have extended our analyzes for heavy quark production in heavy ion collisions and estimated the contribution of the high density effects in this process. Our results have important implications in the signatures of the QCD phase transition, specially in the suppression of quarkonium production since our results indicate that the quarkonium production rate should be strongly modified by the presence of the high density effects. Consequently, if the analyzes of the pA process demonstrate the presence of the these effects in the kinematic regions of RHIC and LHC, we have that the current estimates of quarkonium suppression in AA processes should be completely reanalyzed.

Acknowledgments

The authors acknowledge helpful discussions with M. B. Gay Ducati, J. Jalilian-Marian, M. V. T. Machado and R. Venugopalan. VPG thanks the Brookhaven National Laboratory for its hospitality at a preliminary stage of this work. This work was partially financed by CNPq and FAPERGS, BRAZIL.

References

- [1] Yu. L. Dokshitzer. *Sov. Phys. JETP* **46** (1977) 641; G. Altarelli and G. Parisi. *Nucl. Phys.* **B126** (1977) 298; V. N. Gribov and L.N. Lipatov. *Sov. J. Nucl. Phys* **15** (1972) 438.
- [2] K. J. Eskola, V. J. Kolhinen, C. A. Salgado. *Eur. Phys. J.* **C9** (1999) 61; K.J. Eskola, V. J. Kolhinen, P. V. Ruuskanen. *Nucl. Phys.* **B535** (1998) 351.

- [3] A. H. Mueller, *Nuc. Phys.* **B558** (1999) 285.
- [4] A.L. Ayala, V. P. Gonçalves. *Eur. Phys. J.* **C20** (2001) 343.
- [5] S. Liuti, R. Vogt, *Phys. Rev.* **C51** (1995) 2244.
- [6] N. Hammon *et al.*, *Phys. Rev.* **C59** (1999) 2744.
- [7] M. B. Gay Ducati, V. P. Gonçalves, *Phys. Lett.* **B502** (2001) 92.
- [8] E. Iancu, A. Leonidov, L. McLerran, *Nucl. Phys.* **A692** (2001) 583.
- [9] L. V. Gribov, E. M. Levin, M. G. Ryskin. *Phys. Rep.* **100** (1983) 1; A. H. Mueller, J. Qiu. *Nucl. Phys.* **B268** (1986) 427; I. Balitsky, *Nucl. Phys.* **B463** (1996) 99; A. L. Ayala, M. B. Gay Ducati and E. M. Levin. *Nucl. Phys.* **B493** (1997) 305; *Nucl. Phys.* **B511** (1998) 355; J. Jalilian-Marian, A. Kovner, H. Weigert, *Phys. Rev.* **D59** (1999) 014015; Yu. Kovchegov, *Phys. Rev.* **D60** (1999) 034008.
- [10] A. L. Ayala, M. B. Gay Ducati and E. M. Levin. *Nucl. Phys.* **B493** (1997) 305; *Nucl. Phys.* **B511** (1998) 355.
- [11] S. Frixione *et al.*, *Nucl. Phys.* **B431** (1994) 453.
- [12] See, e. g., M. J. Leich *et al.*, *Nucl. Phys.* **A544** (1992) 197c.
- [13] R. Vogt, *Phys. Rev.* **C61** (2000) 035203.
- [14] M. Gluck, E. Reya and A. Vogt. *Z. Phys.* **C67** (1995) 433.
- [15] M. Gyulassy, L. McLerran, *Phys. Rev.* **C56** (1997) 2219.
- [16] V. P. Gonçalves, *Phys. Lett.* **B495** (2000) 303.
- [17] L. McLerran, R. Venugopalan, *Phys. Rev.* **D59** (1999) 094002.
- [18] F. Gelis and A. Peshier, *Nucl. Phys.* **A697** (2002) 879.
- [19] A. Dumitru, L. McLerran, *Nucl. Phys.* **A700** (2002) 492.
- [20] Conceptual Design for the Relativistic Heavy Ion Collider, BNL-52195, May, 1989; G. Baur *et al.*, CMS Note 2000/060.
- [21] X-N. Wang, M. Gyulassy, *Phys. Rev. Lett.* **68** (1992) 1480.

Figure Captions

Fig. 1: Comparison between the ratio R_G with and without the high density effects for $A=40$ (Ca) and $A=208$ (Pb). The RHIC and LHC kinematic regions are also shown.

Fig. 2: The exponent α [Eq. (4)] as a function of energy \sqrt{s} for two nuclei (Ca and Pb) in pA processes.

Fig. 3: The exponent $\alpha(x_F)$ [Eq. (5)] as a function of x_F for $p - Pb$ processes at RHIC ($\sqrt{s} = 350$ GeV) and LHC ($\sqrt{s} = 8.8$ TeV) ($A=208$) [Note the different inferior limit of the two graphs].

Fig. 4: The exponent β [Eq. (6)] as a function of energy \sqrt{s} for $Pb - Pb$ processes.

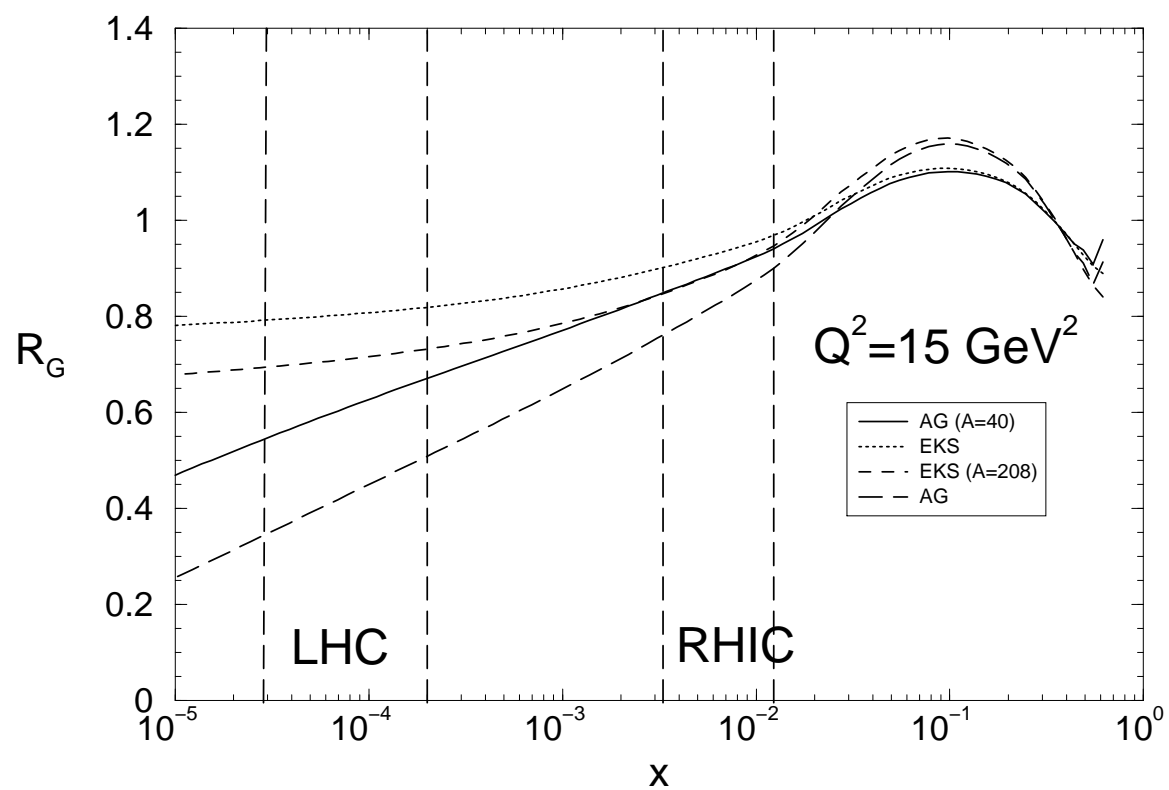


Figure 1:

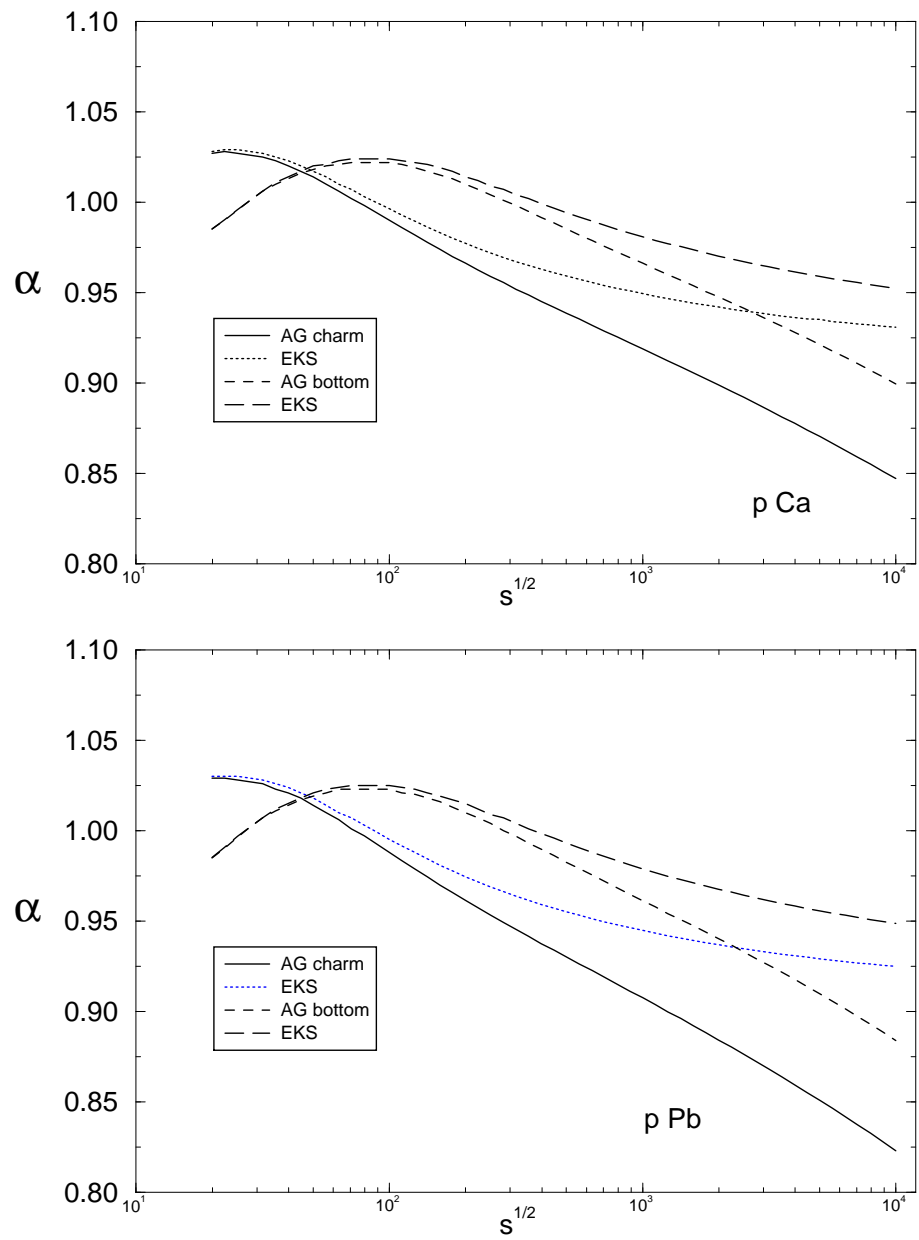


Figure 2:

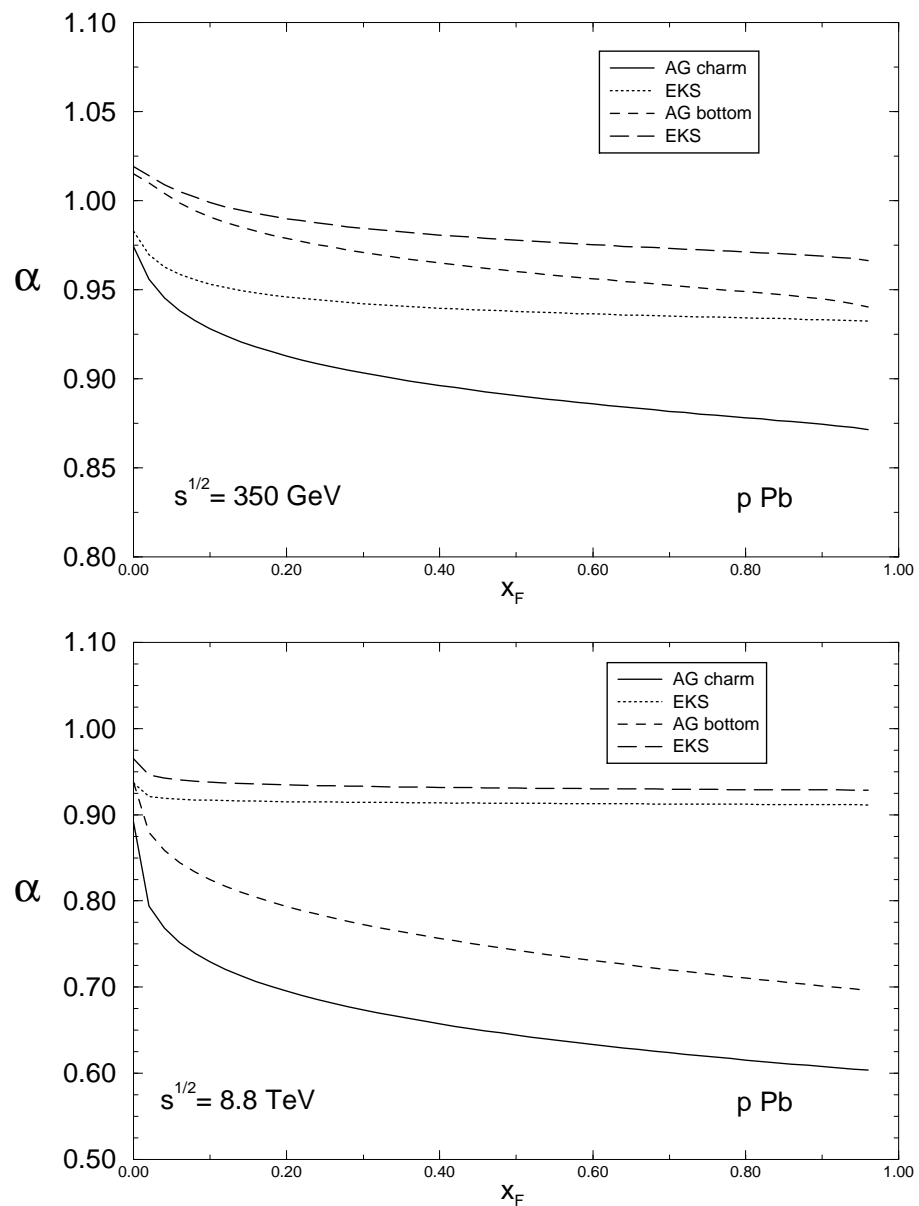


Figure 3:

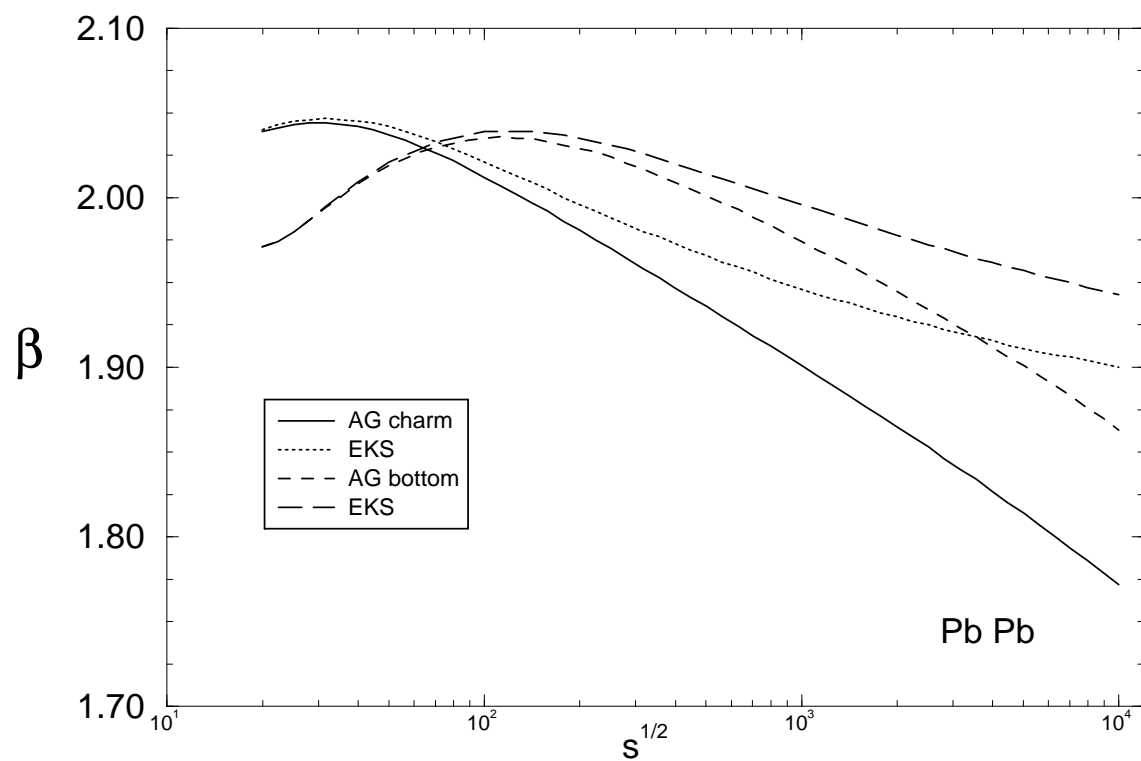


Figure 4: